A STUDY OF IONIZATION ELECTRONS DRIFTING OVER LARGE DISTANCES IN LIQUID ARGON

E. BUCKLEY [2]*, M. CAMPANELLA [3], G. CARUGNO [1], C. CATTADORI [3], A. GONIDEC [1], R. MUÑOZ [1], S. OCHSENBEIN [4], C. RUBBIA [1], D. SCHINZEL [1], W.F. SCHMIDT [1]** and W. SEIDL [1]

[1] CERN, CH 1211, Geneva 23, Switzerland

[2] Laboratori Nazionali dell'INFN, Via Enrico Fermi 40, Frascati, Roma, Italy

[3] Dipartimento di Fisica and Sezione dell'INFN, Università di Milano, Via Celoria 16, Milano, Italy

[4] SIN, 5234 Villigen, Switzerland

We have measured the lifetime of electrons drifting in liquid argon using a gridded ionization chamber with a drift gap of 153 mm. The electrons were produced by the passage of cosmic rays through the chamber We find a best fit for the electron lifetime τ at 5 V/cm of 9.2 ms (with $13.2 > \tau > 7.1$ ms at 95% CL). This value is consistent with all the data below 15 V/cm. This corresponds to an impurity concentration $\rho = 0.03$ ppb oxygen equivalent. The attenuation length calculated from the above lifetime is 18 m for a field of 1 kV/cm. The liquid remained in the chamber for 14 weeks with no recirculation system and suffered no noticeable deterioration with respect to the lifetime or the pulse height. The low field mobility μ_0 has been measured for fields up to 150 V/cm and we find a value of 545 ± 4 cm^2 V^{-1} s^{-1} which is consistent with measurements by other authors. The electron yield as a function of the electric field strength has been measured down to 3 V/cm. The results seem to indicate the need for a modification of the geminate recombination theory.

1. Introduction

The liquid time projection chamber offers the potential for a large continuously sensitive detector with excellent energy and spatial resolution. The use of liquid argon or xenon as the detection media for charged particles is particularly suitable in applications where high density or high mass are required, with the detector acting as a target or a source as in the detection of solar neutrinos or double-beta decay, respectively. Such a detector is planned for the Gran Sasso Underground Laboratory in Italy. The ICARUS detector [1] is a liquid argon TPC designed primarily for studying solar neutrino interactions.

In order to drift electrons over large distances, between 1 and 2 m in the ICARUS detector, the level of electronegative impurities, e.g. oxygen, must be less than 1 ppb and must be maintained at this level over long periods of time. Since the initial proposal for a liquid argon TPC in 1977 [2] a large amount of work has been done to ascertain the feasibility of such a

device [3–8] and the work presented here is part of the continuing development program for the ICARUS experiment.

We have measured the electron lifetime in liquid argon using a gridded ionization chamber with a total volume of 2 l in which electrons produced by the passage of cosmic rays were able to drift over 153 mm in electric fields as low as 3 V/cm, corresponding to a transit time of 9.1 ms. We find that it is possible to achieve the required lifetimes with the use of simple purification system consisting of a mixture of molecular sieve and silica gel together with an Oxisorb cartridge [9] to remove oxygen.

The paper is organized as follows. In section 2 we describe the chamber construction followed by the purification system in section 3. Section 4 deals with the electronics and data acquisition and in section 5 we describe the method used to analyse the pulses obtained and the difficulties involved. Our results are presented in section 6, and section 7 contains concluding remarks.

---

* Visiting Scholar, High Energy Physics Laboratory, Harvard University, Cambridge, MA 02138, USA.
** Visiting scientist 1986/87 from the Hahn–Meitner Institut, Berlin, FRG.

2. The chamber

A cross-section through the chamber is shown in fig. 1. The cathode and the anode were made of disks of

stainless steel 80 mm in diameter and 3 mm thick. The grid was constructed of a mesh of 50 μm diameter stainless steel wires separated by 550 μm. The cathode–grid distance was 153 mm and the grid–anode distance was 4.5 mm. In order to ensure field uniformity, field-shaping rings were placed at intervals of 9 mm between the cathode and the grid, connected to each other by spacers made of insulating material (PTFE). Between each pair of rings a 10 MΩ resistor was placed. The resistors had their outer coating of paint removed and their leads were gold-plated to avoid corrosion during cleaning. The last resistor, placed between the grid and ground, was chosen so that the field between the grid and anode was sufficient to ensure 100% transmission of the electrons through the grid. The grid will be 100% transparent to the drifting electrons if

$$\frac{E_A}{E_B} > \frac{(1+x)}{(1-x)},\tag{1}$$

where E_A is the field after the grid, E_B is the field before the grid and

$$x = \frac{2\pi r}{y},\tag{2}$$

where r is the wire radius and y is the distance between the wire centres [10]. With our values for y and r we

Fig. 1. A cross-section through the chamber.

obtained $E_A > 1.7E_B$ for 100% transparency. The chamber geometry allowed another 10 MΩ resistor to be used, giving $E_A = 2.6E_B$. The shielding inefficiency σ of the grid is given by

$$\sigma = \frac{y}{2\pi p} \ln\left(\frac{y}{2\pi r}\right),\tag{3}$$

where p is the grid–anode distance. The inefficiency is a function of the chamber geometry only and does not depend on the applied field. The inefficiency of the grid was 3%. It should be noted that eqs. (1), (2), and (3) are only exact for a grid of equally spaced parallel wires and hence for a mesh the results are only approximate.

Mounted above and below the main chamber were two parallel plate ionization chambers which served as trigger chambers, providing signals which were put in coincidence to indicate the passage of a cosmic ray muon through the chamber. Each chamber was divided into two 4.5 mm drift gaps by a stainless steel disk of diameter 40 mm. The top plate of the upper drift gap was a stainless steel disk of the same diameter as the cathode and was held at ground. The bottom plate of the lower gap was a grounded cup. This cup prevented the escape of field lines from the trigger chamber electric field to the walls of the chamber vessel and the main drift gap electrodes.

The chamber was mounted on a DN100 ConFlat [11] flange and placed inside a stainless steel container of height 250 mm and diameter 100 mm. The top of the flange contained a single pipe for evacuation and filling of the chamber and the four cryogenic feedthroughs for the chamber readout, trigger chambers and high voltage. The flange was sealed to the container with a copper O-ring and the whole assembly was baked out under vacuum at 100°C for 24 h. A relatively low temperature was used so that the resistors would not be damaged. After these procedures typical leak test rates of 2.7×10^{-9} mbar l s^{-1} were achieved.

3. The purification system

Fig. 2 shows a schematic of the liquid argon purification system. All the metal parts of the system were constructed from stainless steel and were subjected to the CERN "standard cleaning procedure" [12]: (1) washing with detergent at 50°C in a bath equipped with ultrasound; (2) then rinsing with cold demineralised water; (3) washing with demineralised water at 60°C in a bath equipped with ultrasound; and (4) finally degassing in a vacuum oven ($\approx 5 \times 10^{-7}$ Torr) at 950°C. All metal parts, including those of the chamber, underwent this cleaning sequence. The resistors and insulating spacers were subjected to steps 1 through 3. We used all-metal bakeable NUPRO valves [13] with
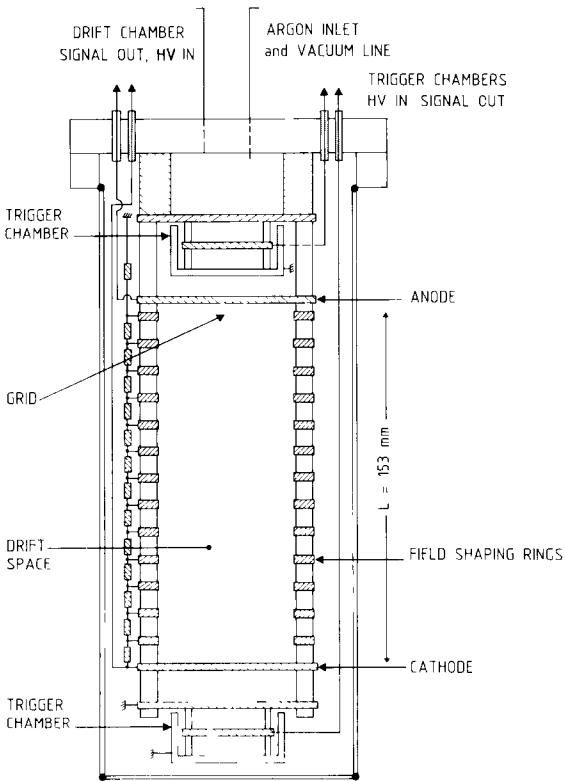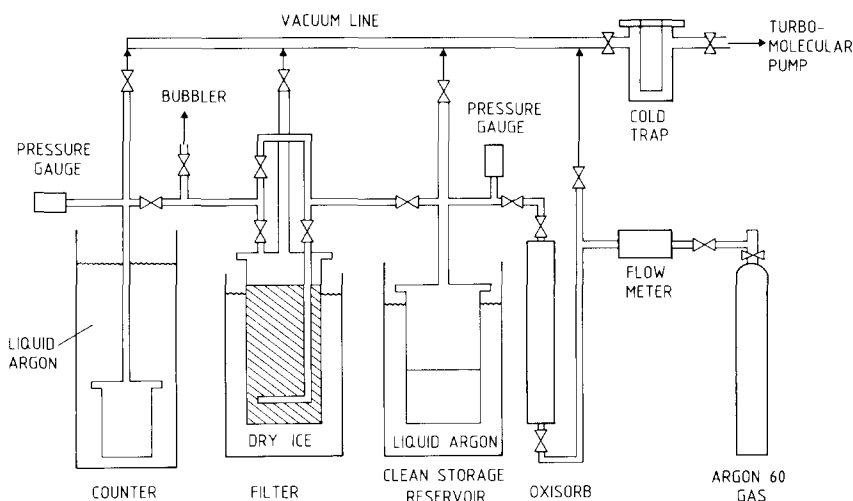
Fig. 2 A schematic of the liquid argon purification system

DN16 ConFlat flanges welded onto each end and connected to the rest of the components with copper O-rings. All connections to the vacuum system were made via vacuum valves with welded bellows.

The system was evacuated using a turbomolecular pump with a liquid nitrogen cold trap placed between the pump and the system to prevent backdiffusion of oil from the pump. The whole assembly was baked out under vacuum at 300°C for 48 h, the final vacuum achieved on the system was 2×10^{-7} mbar and typical leak test rates were 4×10^{-9} mbar l s^{-1}.

The filter consisted of an equal mixture of molecular sieves 4A and 13X [14] and silica gel. The filter was activated under vacuum typically for 12 d at 350°C and a vacuum of 1×10^{-5} mbar on the filter was achieved at this temperature. The silica gel was previously activated in an oven at 250°C for 24 h at atmospheric pressure. During operation the filter was cooled to −70°C using dry ice to increase its adsorption capacity for carbon dioxide and water. Oxygen is not removed by molecular sieves because of its high vapour pressure and nonpolar nature. Instead we use the room temperature getter Oxisorb [9] to ensure its removal. The Oxisorb cartridge is made of chromium embedded in an SiO_2 lattice and adsorbs oxygen by a chemical process rather than a physical one. The reaction which takes place is $2Cr + 3O_2 \rightarrow 2CrO_3$.

The purification of the argon took place in two stages. The starting material was argon 60 gas (99.9999% pure) which had an impurity concentration of about 0.1 ppm of oxygen. The gas was passed through the Oxisorb cartridge with a flow meter placed before it to regulate the speed of the gas flow and so to ensure maximum removal of the oxygen. A typical flow rate was 0.35 l/s. The gas was then liquefied in a clean storage container which was surrounded by a liquid argon bath. The

purpose of this intermediate step was to separate out any fluorinated or chlorinated hydrocarbons which may have been present in the gas bottle from the compressor cycle. It took $2\frac{1}{2}$ h to liquefy 4 l of argon into the storage container.

In the second stage the liquid argon was allowed to boil off and pass through the filter to be liquefied in the chamber. The chamber was also surrounded by a bath of liquid argon. Open dewars were used for the liquid argon baths for ease of refilling as the quantities of argon involved were small. The start of liquefaction in the chamber was indicated by a pressure difference between the filter and the chamber, recorded using the two pressure gauges located as indicated in fig. 2. This pressure difference was kept at 300 mbar during the liquefaction. The end of the liquefaction process was indicated by the equalizing of the pressures on the chamber and storage container and took about $2\frac{1}{2}$ h. In both stages the rate of liquefaction was controlled by the extent of the cold surface seen by the gas as well as by the level of the external liquid argon bath.

Emptying the chamber was carried out by allowing the liquid to boil off and pass through a glass bubbler containing silicon oil. A bubbler was used to prevent backdiffusion of water vapour into the chamber. To empty the chamber in this way took about 2 h.

4. Electronics and data acquisition

A schematic of the readout system is shown in fig. 3. A positive voltage of 1.6 kV was applied to the central plate of each of the trigger chambers, creating an electric field of about 3.6 kV/cm across each of the 4.5 mm gaps. Electrons produced in both of the gaps drifted towards the central plate and the signal was read out
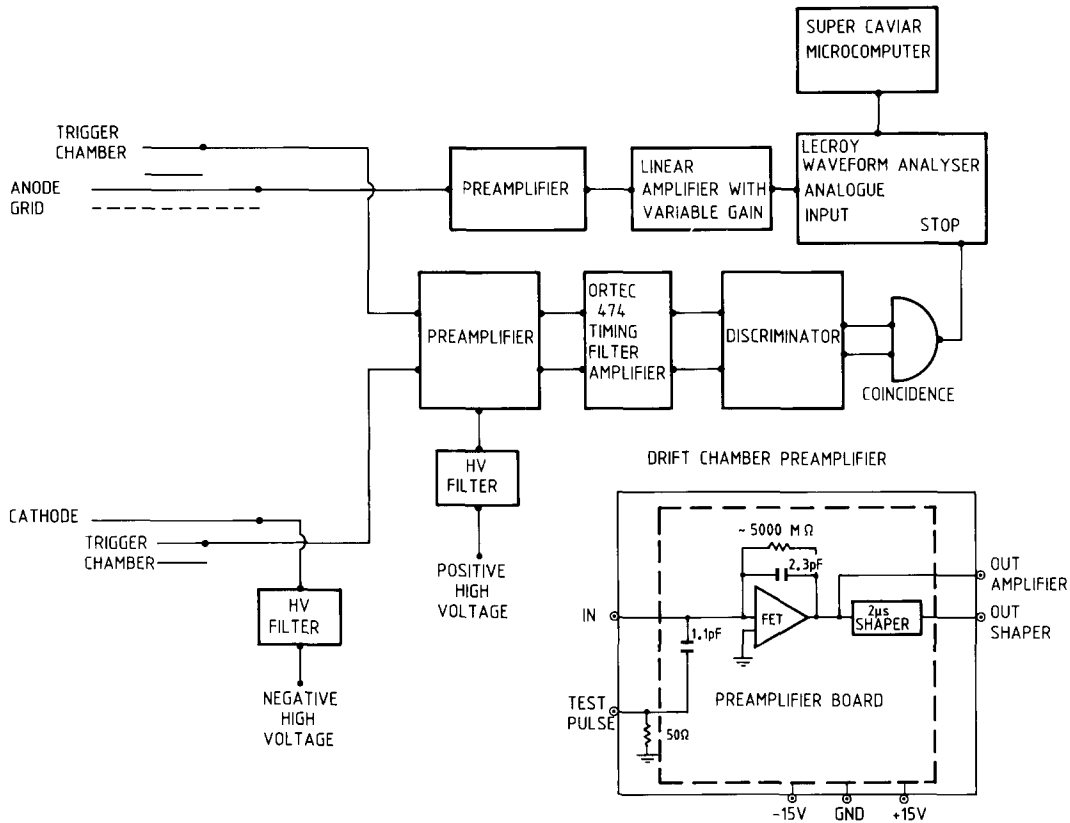
Fig. 3. A schematic of the electronics and readout system.

into a charge-sensitive preamplifier followed by a 500 ns shaper and then an Ortec 474 timing filter amplifier with a gain of two. The signal and high voltage were carried on the same cable and decoupled inside the preamplifier box. The signal from each chamber was sent to a discriminator and the output from the two discriminators was used to generate a coincidence which stopped the conversion of the transient recorder. The discriminator threshold was determined by calculating the expected signal across the two 4.5 mm drift gaps and dividing it by three. As well as triggers from single muons traversing the chamber, electron showers could also produce a trigger due to two particles from the shower, each crossing one trigger chamber at the same time. As the particle had not crossed the whole chamber volume then the pulse height was much lower than the expected pulse height calculated for the 153 mm gap and the transit time was less than t_d. These pulses were removed by an on-line cut on the pulse height. The measured rate of cosmic ray muons which traversed the whole of the chamber length was about 8 events per hour, in agreement with the expected rate of 11 events per hour calculated by taking into account the solid angle of the trigger chambers.

The signal from the main drift chamber was read out using a charge-sensitive preamplifier. A schematic of the preamplifier is shown in fig. 3. Here we did not use any shaping and the feedback time constant of the amplifier was such that long drift times could be recorded without appreciable loss of signal. The noise of the preamplifier was ≈ 0.3 fC. The signal was further amplified by a linear amplifier with variable gain and then fed into the analogue input of a LeCroy 2256 transient recorder. In order to record pulses with very long risetimes, an external clock with a minimum frequency of 80 kHz was used.

The data from the transient recorder were stored on a Super Caviar Microcomputer where they could be viewed on-line and also stored on disk for further analysis. The whole readout chain could be checked by applying a known voltage from a test pulse onto a 1.1 pF test capacitance at the input of the preamplifier.

5. Analysis of pulse shapes

The passage of a cosmic ray through the chamber leaves a track of uniform ionization in the form of

electron–positive ion pairs. The electrons then move under the influence of an applied electric field and after passing through the grid they induce a signal on the anode. The contribution to the current from the positive ions can be neglected as their mobility is orders of magnitude less than the electron mobility.

The effect of a grid is to shield the anode from the drifting electrons so that a signal is induced on the anode only after the electrons have crossed the grid. Each electron drifts the same distance across the grid–anode gap before collection hence the total charge collected Q_0 will be $N_0 e$ (c.f. the parallel plate chamber where the total charge collected is $N_0 e/2$). Note that the transit time t_d is determined by the cathode–grid distance which is long compared to the grid–anode distance. The current as a function of time $i(t)$ measured at the anode is determined by the speed $v_d = d/t_d$ with which the electrons arrive at the grid. This is the case because once the electrons have traversed the grid they come into a region of higher field strength and they cross the much shorter grid–anode gap in a drift time t_d' which is much less than t_d. The current detected at time t namely $i(t)$ is given by

$$i(t) = Ne\frac{v_d}{d},\tag{4}$$

where N is the number of electrons contributing to the current pulse.

If electron attaching impurities are present then not all of the electrons will arrive at the grid–anode gap. A certain fraction are converted into negative ions of much smaller mobility and are thus lost for the electronic pulse. The electron attachment to an impurity S can be described by the following reaction

$$e^- + S \underset{k_S}{\rightarrow} S^-,\tag{5}$$

where the rate constant k_S is given by

$$k_S = \int v\sigma(v)f(v)\,dv,\tag{6}$$

where v is the electron velocity, $f(v)$ is the velocity distribution of the electrons and $\sigma(v)$ is the cross-section as a function of velocity for interaction of the electrons with impurity S. If instead the cross-section is expressed as a function of energy then

$$k_S = \int \sigma(E)f(E)\,dE,\tag{7}$$

where $f(E)$ is the well-known Maxwell distribution function. For oxygen the rate constant in liquid argon has been measured and is found to decrease with increasing electric field [15].

Under the assumption that the number of electrons N produced by the passage of an ionizing particle is

smaller than the impurity concentration N_S, the number of electrons lost per time interval is

$$\frac{dN}{dt} = -k_S N_S N.\tag{8}$$

For hermetically sealed containers which have been properly cleaned before filling with liquid N_S remains constant and integration of eq. (8) gives

$$N = N_0\,e^{-t/\tau},\tag{9}$$

where τ is the electron lifetime and is related to the rate constant and the impurity concentration by

$$\tau = \frac{1}{k_S N_S}.\tag{10}$$

Substituting for N in eq. (4) we obtain

$$i(t) = N_0\,e^{-t/\tau}e\frac{v_d}{d},\tag{11}$$

and after integration

$$Q(t) = \frac{N_0 e\tau}{t_d}(1 - e^{-t/\tau}).\tag{12}$$

This ideal pulse shape is modified by the electronics chain and this effect has to be fully taken into account when fitting the pulses to extract the lifetime. In our case the response $R(t)$ of the electronics can be represented as the sum of three terms:

$$R(t) = A_1\,e^{-t/\tau_1} + A_2\,e^{-t/\tau_2} + A_3\left(\frac{t}{\tau_3}\right)e^{-t/\tau_3}\tag{13}$$

where $A_1 = 0.77$, $\tau_1 = 4.63$ ms, $A_2 = 0.14$, $\tau_2 = 0.30$ ms, $A_3 = 0.87$, $\tau_3 = 4.11$ ms. The constants A_n and τ_n were obtained by fitting the response of the electronics to a test pulse in the form of a step function [16].

The charge collected at time t, where $t \leq t_d$ is then given by

$$Q(t) = \frac{N_0 e}{t_d}\int_0^t e^{-\theta/\tau}R(t-\theta)\,d\theta.\tag{14}$$

To avoid introducing uncertainties due to calibration of the electronics and the poor theoretical knowledge of the electron yield at low fields in liquid argon, we have used the ratio between the charge collected at time t and the maximum charge, $Q(t)/Q_{max}$, as the quantity to be fitted to determine the electron lifetime. The pulses were fitted for the parameter τ using the shape described by eq. (15):

$$\frac{Q(t)}{Q_{max}} = \frac{\int_0^t e^{-\theta/\tau}R(t-\theta)\,d\theta}{\int_0^{t_{max}} e^{-\theta/\tau}R(t_{max}-\theta)\,d\theta}.\tag{15}$$

The minimization program MINUIT [17] was used and the χ^2 was minimized by varying τ.

This method is most sensitive if the electron lifetime is less than the transit time across the chamber. Fig. 4
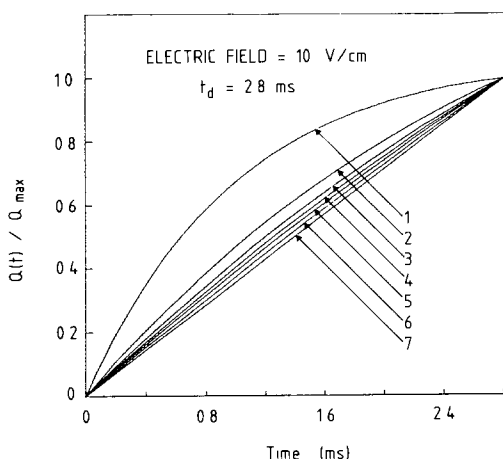
Fig. 4. The theoretical pulse shapes for seven values of τ at $E = 10$ V/cm, demonstrating the difficulty in accurately determining τ if it is longer than the drift time. The curves are (1) $\tau = 1$ ms, (2) $\tau = 3$ ms, (3) $\tau = 5$ ms, (4) $\tau = 7$ ms, (5) $\tau = 10$ ms, (6) $\tau = 20$ ms, (7) $\tau = \infty$.

illustrates the difficulty of distinguishing between different lifetimes once τ becomes greater than the transit time. The theoretical pulse shapes for $Q(t)/Q_{max}$ are shown for seven different lifetimes ($\tau = 1, 3, 5, 7, 10, 20, \infty$ ms), demonstrating that it is possible to distinguish between 1 and 3 ms but it becomes harder as τ increases beyond the drift time of 2.8 ms. At very low fields the transit time is sufficiently long that acoustic noise becomes a problem which is difficult to eliminate. Noise superimposed on the pulse can distort the shape leading to a lengthening or shortening of the measured lifetime.

6. Results

Cosmic ray muon data were taken for a number of electric fields ranging from 3 up to 230 V/cm, and the raw data for four typical pulses are shown in fig 5. Note the rounding of the pulses and decrease in pulse height as the electric field decreases, due to the effect of electron attachment and also amplifier response.

For the determination of the lifetime we have used the pulses taken at low fields as these will be most sensitive to the effects of electron attachment. Taking the data at 5 V/cm and using the method in section 5 we obtain $\tau = 9.2^{+3.4}_{-1.8}$ ms ($13.2 > \tau > 7.1$ ms at 95% CL). We then check that this value of the lifetime gives consistent results for the pulses recorded at other fields. We find that a lifetime of 9.2 ms gives a good description of the data for all fields for which pulse shapes were recorded (up to 15.2 V/cm). This can be seen in fig. 6 where we show four pulses taken at different

fields together with the curves calculated using $\tau = 9.2$ ms.

The liquid was kept in the chamber for 14 weeks with no recirculation system and we observed no noticeable deterioration in the measured lifetime or the pulse height, as is demonstrated in fig. 7 where the measured pulse height is plotted as a function of time after filling of the chamber.
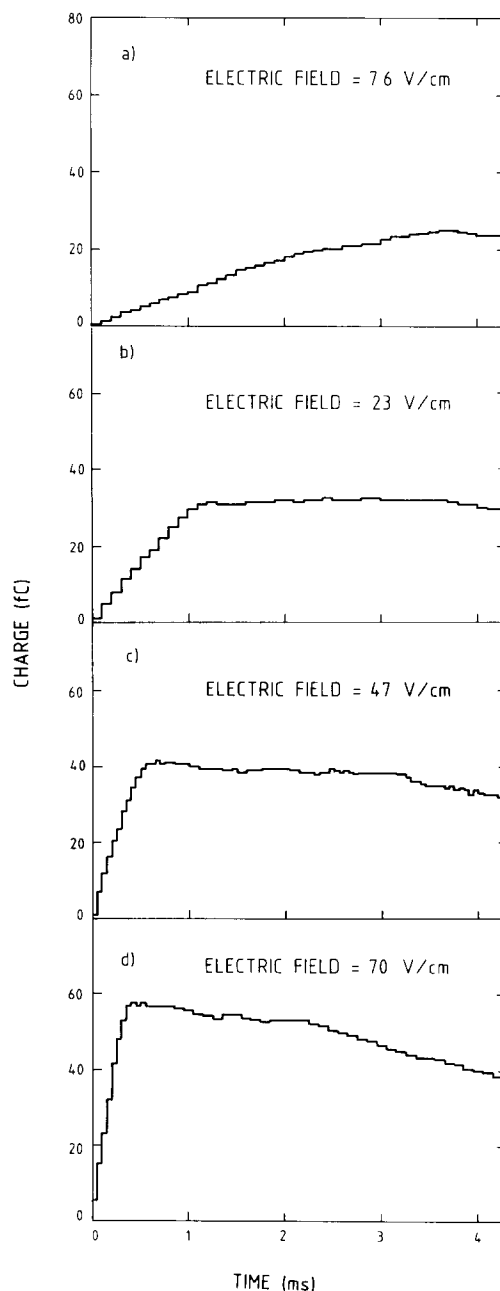

Fig. 5. Typical pulses for four electric fields; (a) 7.6 V/cm, (b) 23 V/cm, (c) 47 V/cm and (d) 70 V/cm.

We have used our measurement of τ to determine the attenuation length λ which is related to τ by the drift velocity v_d by
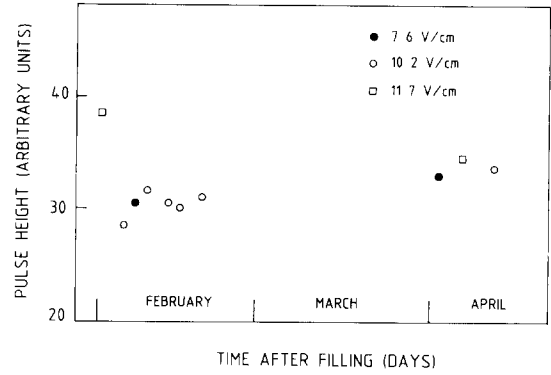
$$\lambda = v_d \tau. \tag{16}$$

Fig. 7. The measured pulse height as a function of time after filling of the chamber.

For a field of 5 V/cm and $\tau = 9.2$ ms we obtain $\lambda = 25$ cm (using the value for μ_0 of 545 cm^2 V^{-1} s^{-1} obtained below). For a field of 1 kV/cm (which is the design field for ICARUS [1]) with $v_d = 2 \times 10^5$ cm s^{-1} we obtain

$$\lambda = 18 \text{ m}. \tag{17}$$

We can use eq. (10) to determine the impurity concentration N_S in mole/l, assuming that all of the impurity is oxygen. For the rate constant at 5 V/cm we use $k_S \approx 10^{11}$ l mole^{-1} s^{-1} from ref. [15] and with $\tau = 9.2$ ms we obtain $N_S = 1.0 \times 10^{-9}$ mole/l. The concentration N_S is related to the concentration ρ in ppb by

$$\rho = N_S/N_{AR}, \tag{18}$$

where N_{AR} is the number of moles in 1 litre of liquid argon. Substituting for N_S in eq. (18) and using $N_{AR} = 35$ we obtain

$$\rho = 0.03 \text{ ppb}, \tag{19}$$

where ppb is defined as one oxygen molecule in every 10^9 argon atoms.

The drift velocity v_d at low fields, $E \leq 150$ V/cm, is related to the electric field E by

$$v_d = \mu_0 E, \tag{20}$$

where μ_0 is the low field electron mobility. Using data taken at different fields we can measure the drift velocity and hence determine μ_0. This measurement is only valid if $\tau \gg t_d$ so that the effects of electron attachment (and amplifier response) can be neglected. Fig. 8 shows the measured drift velocity as a function of the applied field. We know that the lifetime is long so we use all data below 150 V/cm and assuming eq. (20) we obtain a value for the mobility of (545 ± 4) cm^2 V^{-1} s^{-1} for a temperature of 86.8 K. (If we adopt a conservative approach of only using the data above 10 V/cm then we obtain (542 ± 4) cm^2 V^{-1} s^{-1}.) The curve in fig. 8 is obtained from eq. (20) using $\mu_0 = 545$ cm^2 V^{-1} s^{-1}.

Fig. 6. Averaged pulses for (a) 5.03 V/cm, (b) 7.6 V/cm, (c) 9.9 V/cm and (d) 10.23 V/cm together with the calculated curves for $\tau = 9.2$ ms.
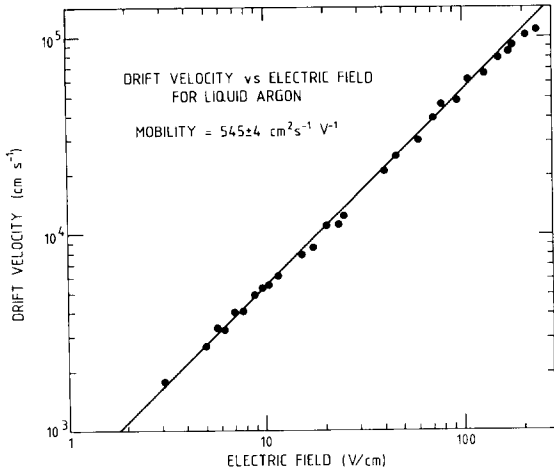
Fig. 8. The electron drift velocity v_d in cm s^{-1} as a function of electric field E in V/cm. The solid line is obtained from $v_d = \mu_0 E$ with $\mu_0 = 545$ cm^2 V^{-1} s^{-1}.

Our measurement is in good agreement with those of other groups [18–22].

The measurement of the charge $Q(t_d)$ at lifetime τ enables us to extract the initial charge $Q_0 = N_0 e$ as a function of the electric field E. We assume that the maximum charge is collected at the drift time t_d, this is reasonable as we know that $\tau \gg t_d$, and for each field we determine the pulse height spectrum. The mean value in ADC counts is determined by fitting a Gaussian to the spectrum and this mean pulse height is then transformed into fC by applying the appropriate calibration constants. The error on the charge calibration is estimated to be 10–20% due to the uncertainty in the exact value of the test capacitance. We then use eq.
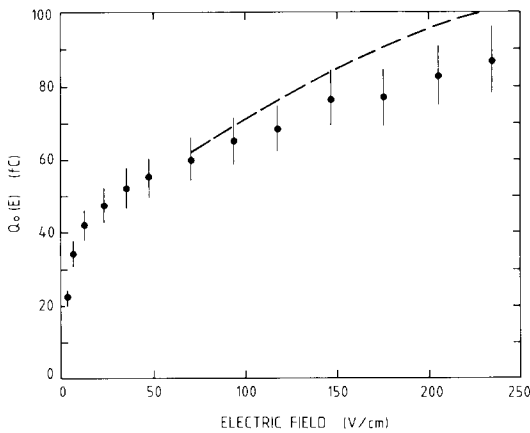

Fig. 9. The initial charge $Q_0(E)$ deposited in the chamber by the passage of a cosmic ray as a function of the electric field E. The error bars indicate the effect of a $\pm 10\%$ systematic error in the charge determination. The dashed line is calculated from the data of ref. [24].

(14) with $t = t_d$ to correct for the effect of electron attachment and amplifier response and obtain $Q_0(E)$ in fC, shown in fig. 9 as a function of E. The effect of a $\pm 10\%$ systematic error on the charge calibration is indicated by the error bars.

The dependence of the electron yield on the electric field is usually explained by making use of Onsager's treatment of the escape probability for a single ion pair separated by a distance r [22]. The electron yield has been calculated using Onsager's theory [23]. It is found that for field strengths of up to a few hundred V/cm in liquid argon the electron yield is a linear function of the field strength and the slope is determined by the absolute temperature T and the relative dielectric constant ϵ_r only. The charge $Q_0(E)$ can be expressed as

$$Q_0(E) = Q_0(E=0)(1 + \alpha E), \qquad (21)$$

where $Q_0(E = 0)$ is the number of electrons that escape recombination with positive ions in the absence of an external electric field. The slope α is given by

$$\alpha = \frac{er_c}{2k_B T}, \qquad (22)$$

where r_c is the critical Onsager radius, given by the condition that at this separation distance the Coulomb energy of the ion pair is equal to $k_B T$, and can be written as

$$r_c = \frac{e^2}{4\pi\epsilon_r \epsilon_0 k_B T}. \qquad (23)$$

Comparison of eq. (21) with the data shows significant deviations pointing towards an inapplicability of the Onsager treatment to liquid argon. The predicted slope/intercept ratio is 8.4×10^{-4} cm V^{-1} whereas that measured from fig. 9 is $\approx 3.28 \times 10^{-3}$ cm V^{-1}. This discrepancy has previously been noticed by other authors. The dashed line in fig. 9 has been calculated from the data of ref. [24]. The two measurements agree reasonably well within our quoted systematic errors.

We believe that the basic mechanism underlying this behaviour is the following. In liquid argon the energy required to create one electron–ion pair is 23.6 eV (corresponding to 4.2 electrons per 100 eV of deposited energy) and for minimum ionizing particles $dE/dx = 2.1$ MeV/cm. Hence the average initial separation distance r_0 between ionization events, i.e. between the positive ions, is ≈ 1100 Å. Using eq. (23) with $\epsilon_r = 1.52$ and $T = 87$ K we obtain $r_c = 1261$ Å, hence the ionization events overlap because $r_c \approx r_0$. Therefore even if the electron thermalizes at a distance $r > r_c$ and hence escapes recombination with its parent ion it may still recombine with another ion. Consequently the Onsager model does not apply as it assumes that the electron–ion pair is isolated and this does not appear to be the case in liquid argon. This behaviour will clearly lead to increased recombination at low electric fields. We note

here that two independent theoretical calculations are currently underway to explain this discrepancy [25,26].

7. Conclusions

We have measured the lifetime of electrons drifting in liquid argon and we find that $\tau = 9.2$ ms. This corresponds to an impurity concentration of $\rho = 0.03$ ppb oxygen equivalent and an attenuation length of 18 m at 1 kV/cm, clearly well within the design specifications of the ICARUS [1] detector which will operate with a field of 1 kV/cm over a drift-gap of several metres.

The results demonstrate the difficulty of measuring lifetimes which are long compared to the transit time across the chamber at the lowest fields attainable. This situation could be improved by using a longer chamber which allowed the electrons to become attached to impurities even at moderate electric fields. Clearly for very long chambers the use of cosmic rays as the source of ionization becomes impractical and an alternative source of ionization must be used, e.g., laser or radioactive sources.

The long lifetimes obtained suggest that a simple purification system is capable of producing liquid argon of the quality required for the ICARUS [1] detector.

Finally, measurements of the electron yield at low electric field strength are of importance for the development of a theory for the behaviour of minimum ionizing particles at low fields in liquid argon.

Acknowledgements

References

[1] ICARUS proposal CERN–Harvard–Milano–Padova–Roma–Tokyo–Wisconsin Collaboration, INFN/AE-85/7 Frascati (1985).

[2] C. Rubbia, CERN-EP Internal Report 77-8 (1977) unpublished.

[3] H.H. Chen and J.F. Lathrop, Nucl. Instr. and Meth. 150 (1978) 585.

[4] H.H. Chen and P.J. Doe, IEEE Trans. Nucl. Sci. NS-28 (1981) 454.

[5] P.J. Doe, H.J. Mahler and H.H. Chen, Nucl. Instr. and Meth. 199 (1982) 639.

[6] K. Deiters et al., Nucl. Instr. and Meth. 180 (1981) 45.

[7] E. Gatti, S. Padovini, L. Quartapelle, N.E. Greenlaw and V. Radeka, IEEE Trans. Nucl. Sci. NS-26 (2) (1979) 2910.

[8] E. Aprile, K.L. Giboni and C Rubbia, Nucl. Instr. and Meth. A241 (1985) 62.

[9] Messer Griesheim GmbH, Oxisorb Gas Purifying System.

[10] O. Bunemann, T.E. Cranshaw and J.A. Harvey. Can. J. Res. 27 (1949) 191.

[11] ConFlat is a trademark of Varian, USA.

[12] This procedure was originally developed for the cleaning of the stainless steel vacuum elements of the CERN Intersecting Storage Rings. See A.G. Mathewson, CERN-ISR-VA 74-10, unpublished.

[13] NUPRO valves are manufactured by the NUPRO Company, Ohio, USA.

[14] Union Carbide Corp., 4A and 13X molecular sieves.

[15] G. Bakale, U. Sowada and W.F Schmidt, J. Phys. Chem. 80 (1976) 2556.

[16] UA1 Technical Note UA1/TN 86-85 (1986) unpublished.

[17] MINUIT Function Minimization and Error Analysis, CERN Program Library.

[18] K. Yoshino, U. Sowada and W.F. Schmidt, Phys. Rev. A14 (1976) 438.

[19] E. Shibamura et al., Nucl. Instr. and Meth. 131 (1975) 131.

[20] L.S Miller, S. Howe and W.E. Spear, Phys. Rev. 166 (1968) 871.

[21] B. Halpern, J. Lekner, S. Rice and R. Gomer, Phys Rev. 156 (1967) 351

[22] E.M. Guschchin, A.A. Kruglov and I.M. Obodovskii, Zh Eksp. Teor. Fiz. 82 (1982) 1114; L. Onsager, Phys. Rev. 54 (1938) 554.

[23] J. Sass, private communication.

[24] R.T. Scalettar, P.J Doe, H.J. Mahler and H.H. Chen, Phys. Rev. A25 (1982) 2419.

[25] A. Mozumder and W.G. Burns, 9th Int. Conf. on Cond. and Breakdown in Diel Liqu., Salford, July 1987, IEEE Publication No 87 CH2403-4, pp. 99–102.

[26] M. Tachiya, Rad. Phys. Chem. 30 (1987) 75.